Evaluation of Pediatric Near-Infrared Cerebral Oximeter for Cardiac Disease

Renee N. Kreeger, MD, Chandra Ramamoorthy, MBBS, FRCA (UK), Susan C. Nicolson, MD, Warwick A. Ames, MBBS, FRCA, Russel Hirsch, MD, Lynn F. Peng, MD, Andrew C. Glatz, MD, Kevin D. Hill, MD, Joan Hoffman, MD, Jon Tomasson, MD, and C. Dean Kurth, MD

Departments of Anesthesia and Cardiology, Cincinnati Children's Hospital Medical Center, Cincinnati, Ohio; Departments of Anesthesia and Cardiology, Stanford University Medical Center/Lucile Packard Children's Hospital, Stanford, California; Divisions of Cardiothoracic Anesthesia and Cardiology, The Children's Hospital of Philadelphia, Philadelphia, Pennsylvania; Departments of Anesthesia and Pediatric Cardiology, Duke University Medical Center, Durham, North Carolina; and Department of Pediatric Cardiology, Rush University Medical Center, Chicago, Illinois

Background. **Cerebral hypoxia-ischemia remains a complication in children with congenital heart disease. Near-infrared spectroscopy can be utilized at the bedside to detect cerebral hypoxia-ischemia. This study aimed to calibrate and validate an advanced technology near-infrared cerebral oximeter for use in children with congenital heart disease.**

Methods. **After institutional review board approval and parental consent, 100 children less than 12 years and less than 40 kg were enrolled. Phase I (calibration) measured arterial and jugular venous saturation (SaO_2, SjO_2) by co-oximetry simultaneously with device signals to calibrate an algorithm to determine regional cerebral saturation against a weighted average cerebral saturation ($0.7\ SjO_2 + 0.3\ SaO_2$). Phase II (validation) evaluated regional cerebral saturation from the algorithm against the weighted average cerebral saturation by correlation, bias, precision, and $A_{Root\ Mean\ Square}$ assessed by linear regression and Bland-Altman analysis.**

Results. **Of 100 patients, 86 were evaluable consisting of 7 neonates, 44 infants, and 35 children of whom 55% were female, 79% Caucasian, and 41% with cyanotic disease. The SaO_2 and regional cerebral saturation ranged from 34% to 100% and 34% to 91%, respectively. There were no significant differences in subject characteristics between phases. For the entire cohort, A_{RMS}, bias, precision, and correlation coefficient were 5.4%, 0.5%, 5.39%, and 0.88, respectively. Age, skin color, and hematocrit did not affect these values.**

Conclusions. **This cerebral oximeter accurately measures the absolute value of cerebral saturation in children over a wide range of oxygenation and subject characteristics, offering advantages in assessment of cerebral hypoxia-ischemia in congenital heart disease.**

(Ann Thorac Surg 2012;94:1527–33)

Neurocognitive and behavioral disabilities have been long recognized in children with congenital heart disease (CHD). A recent case control study found a stroke rate of 0.54% [1], while a single center review estimates the postoperative seizure rate at 2.3% [2]. Neurologic complications after congenital heart surgery occur in up to 25% of patients [3]. Although the etiologies of these disabilities are multifactorial, involving genetic and perioperative conditions, cerebral hypoxia-ischemia has been identified as a contributor, especially in children with complex cardiac anomalies [4]. Detection of cerebral hypoxia-ischemia remains difficult in infants, as conventional techniques such as neurologic exam, electroencephalography, jugular bulb oximetry, and magnetic resonance imaging are unreliable or impractical. Real-time, bedside diagnosis of hypoxia-ischemia could permit interventions to potentially improve neurodevelopmental outcomes.

Near−infrared spectroscopy (NIRS) is a noninvasive, portable technology similar to pulse oximetry, which monitors oxygenation in the brain, muscle, and other organs to detect tissue hypoxia-ischemia in real-time [5–10]. It uses near-infrared light (700 to 900 nm) and hardware similar to pulse oximetry to monitor the tissue bed beneath the sensor containing a mixed vascular oxygen saturation dominated by small gas-exchanging vessels (arterioles, capillaries, and venules) [9]. At present, there are 2 commercially available NIRS devices, INOVS (Covidien Corporation [formerly Somanetics], Troy, MI) and FORE-SIGHT (CAS Medical Systems [CASMED], Branford, CT), that are cleared by the Food and Drug Administration (FDA) for use in pediatrics and adults. These 2 devices differ with respect to design, hardware, and algorithm to determine regional cerebral

Accepted for publication May 11, 2012.

Presented at the Late-Breaking Clinical Trial Abstract Session on Congenital Heart Surgery at the Forty-eighth Annual Meeting of The Society of Thoracic Surgeons, Fort Lauderdale, FL, Jan 28–Feb 1, 2012.

Address correspondence to Dr Kreeger, Cincinnati Children's Hospital Medical Center, 3333 Burnet Ave, Cincinnati, OH 45229; e-mail: renee.kreeger@cchmc.org.

0003-4975/$36.00
http://dx.doi.org/10.1016/j.athoracsur.2012.05.096

Abbreviations and Acronyms

A_{RMS} = accuracy root mean square
ASA = American Society of Anesthesiologists
CHD = congenital heart disease
ECMO = extracorporeal membrane oxygenation
FDA = Food and Drug Administration
NIRS = near infrared spectroscopy
rScO2 = calculated regional cerebral oxygen saturation
SaO_2 = arterial hemoglobin oxygen saturation
$SavO_2$ = arteriovenous oxygen saturation
SjO_2 = jugular bulb venous oxygen saturation
SpO_2 = oxygen saturation (from pulse oximetry)
SvO_2 = venous hemoglobin oxygen saturation

oxygen saturation ($rScO_2$), and possess limitations. The Covidien device was cleared to monitor changes in $rScO_2$ in infants and children, whereas the CASMED device measures absolute $rScO_2$ but was validated in a narrow patient population [11]. Recently, Nonin Medical, Inc (Plymouth, MN) developed a NIRS device (EQUANOX) cleared by the FDA for use in adults and children greater than 40 kg. This device utilizes a dual-emitter/dual-detector sensor and dynamic compensatory algorithms which more effectively eliminate scalp and skull contamination to focus on brain tissue and automatically adjust for variations in tissue optical properties to improve accuracy over a wide range of age and physiologic condition.

The purpose of this study was to calibrate (phase I) and validate (phase II) the Nonin NIRS EQUANOX device with a new small sensor to measure $rScO_2$ in children less than 40 kg with cardiovascular disease undergoing cardiac catheterization.

Patients and Methods

After Institutional Review Board approval, informed parental consent, and patient assent as appropriate, children less than 12 years old and less than 40 kg with cardiovascular disease scheduled for cardiac catheterization were eligible. Patients with CHD display a range of arterial hemoglobin oxygen saturation (SaO_2), typically from 70% to 100%, and thus jugular bulb hemoglobin oxygen saturation (SjO_2) and $rScO_2$ vary over a range. Exclusion criteria included the following: preexisting allergies to Nonin sensor adhesive; a skin condition at the sensor site; craniofacial disease preventing forehead application of the sensor; hemoglobinopathy; cerebrovascular disease including previous extracorporeal membrane oxygenation (ECMO); inability to lie supine with neutral neck position during catheterization for fluoroscopy to confirm catheter placement in the jugular bulb; acute neurologic injury within 10 days; a structural brain lesion beneath the sensor; or an emergent, life-threatening condition impacting study conduct.

We investigated the EQUANOX Regional Oximeter System (Nonin Medical Inc) using the pediatric sensors designed for neonates, infants, and children less than 40 kg; the EQUANOX 8004CB (adhesive) and EQUANOX 8004CB-NA (nonadhesive), which were not cleared by the FDA at the time of the study. The device system consisted of a laptop computer connected to a serial to universal serial bus convertor and interface box linked to four oximeter devices (pods, Model 7600PA) attached to four optical sensors. The pediatric sensor consists of a thin, soft, flexible polymer (2.5 mm $\times$ 39 mm $\times$ 54 mm) embedded with two light emitting diodes and two photodiode detectors. Each light emitting diode incorporates four wavelengths; 730 nm, 760 nm, 810 nm, and 880 nm. This dual emitter-dual detector sensor architecture allows for two short light paths through scalp and skull and two long light paths through brain tissue. The source-detector separations were 1.25 cm and 2.5cm.

One hundred neonates (0 to 30 days), infants (31 days to 2 years), and children (2 to 12 years) were enrolled. Patients received anesthesia and cardiac care as directed by their attending physicians. After anesthesia induction but before cardiac catheterization, sensors were placed on the forehead bilaterally below the hairline and above the supraorbital ridge. Good sensor contact was ensured by gentle pressure to the adhesive sensor and by head wrap for the nonadhesive sensor.

After sensor placement, the cardiologist inserted femoral arterial and venous catheters unless catheters were in situ. The venous catheter was directed to the superior vena cava into the jugular bulb by fluoroscopy with the tip at the cervical spine (C1-C3). After patient stability, arterial and jugular bulb venous samples were drawn simultaneously over 15 seconds and the event was marked electronically. Samples were immediately injected into a co-oximeter (Rapidpoint 405; Siemens Healthcare Diagnostics, Tarrytown, NY) to measure concentrations of total hemoglobin, fractional oxygen, oxygen content, carboxyhemoglobin, methemoglobin, oxyhemoglobin saturation, as well as blood gases, and pH. In neonates, total bilirubin concentration was measured. The jugular bulb catheter was then withdrawn to the superior vena cava, and the catheterization proceeded.

Data were analyzed with statistical analysis software (SAS 9.1; SAS Institute, Cary, NC). Analyses were performed directly from the data collection system data files.

The study sample size was determined with the following assumptions: (1) arterial and venous saturation were 87.5 $\pm$ 6.25 and 62.5 $\pm$ 6.25, respectively; (2) $rScO_2$ has the same mean as $SavO_2$ with 50% increase in standard deviation; (3) 2-sided 95% confidence intervals will be generated; and (4) 80% power is sufficient. A sample size of 40 patients was calculated for each phase. One hundred patients were enrolled to accommodate a loss of 20% of patients.

The cerebral circulation contains arteries, capillaries, and veins. Distribution of blood in these beds varies somewhat among patients and by measurement method [12]. To approximate the cerebral circulation measured by NIRS, jugular venous hemoglobin-O2 saturation ($SavO_2$) is used, defined by $SavO_2 = r\ (SvO_2) + (1\text{-}r)$

(SaO_2), where r is the fraction of venous volume and 1-r is the arterial fraction. Venous and arterial volume fractions are, respectively, 0.70 to 0.85 and 0.30 to 0.15 [11–13]. In this study, an r of 0.70 was chosen for consistency with other NIRS device studies. The $rScO_2$ was calibrated using a 4-wavelength Beer-Lambert formulation, where extinction coefficients were chosen by minimizing the mean square error between $rScO_2$ and $SavO_2$. Measures of accuracy include accuracy root mean square (A_{RMS}), mean bias, precision, intercept, slope, and Pearson correlation. The A_{RMS} between $rScO_2$ and $SavO_2$ is presented with the 95% bias-corrected adjusted bootstrap confidence interval from 2,000 bootstrap samples [14]. Precision is presented with the 95% confidence interval based on the uniformly most powerful unbiased test [15]. The Pearson correlation coefficient is presented with its 95% confidence interval using a Fisher z transformation. Device accuracy was determined primarily through the A_{RMS} statistic, which estimates agreement between a test and reference device. The device was considered accurate if A_{RMS} was less than 6%. Least squares linear regression analysis and Bland-Altman analysis were performed to assess correlation and limits of agreement [16, 17].

Results

Of 100 consented patients, 86 were included in the analysis. Fourteen subjects were excluded due to lack of venous access (4), incorrect sample processed (1), no blood samples (2), sample processed late (1), co-oximeter error (2), device malfunction (1), jugular bulb catheter below C3 (1), patient instability (1), and right subdural hematoma (1). Eighty-nine percent of patients were American Society of Anesthesiologists (ASA) physical status 3 and 4. Sixty-two percent of patients had cyanotic defects, 15% had obstructive defects, 8% had septal defects, 7% had pulmonary hypertension without structural heart disease, 6% had an isolated patent ductus arteriosus, and 2% had cardiomyopathy. Patients received general anesthesia maintained with intravenous propofol with or without ketamine infusions (56%), with inhalation of sevoflurane or isoflurane (40%), or with a combination of intravenous and inhaled agents (4%).

Patient demographics did not differ between calibration and validation phases (Table 1). Ages ranged from 4 days to 11 years, a majority being neonates and infants (59%) and Caucasian (79%), although 28% were of darker complexion. The room air pulse oximetry (SpO_2) was less than 80% in 16% of patients, less than 90% in 25%, and ranged from 66% to100%. Bilirubin ranged from 0.2 to 6.2 mg/mL.

Arterial and venous co-oximetry values were similar in phases I and II (Table 2) except for arterial pO_2 ($p = 0.014$), arterial hematocrit ($p = 0.0038$), and arterial saturation ($p = 0.0050$), which were greater in phase I patients. As expected, arterial and venous values varied among patients; arterial pCO_2 ranged from 28 to 61 mm Hg, arterial pO_2 ranged from 25 to 131 mm Hg, total hemoglobin (tHb) ranged from 8 to 23 g/dL, and SaO_2 ranged from 34% to 100%. There was no appreciable carboxyhemoglobin or methemoglobin.

Ipsilateral and contralateral $rScO_2$ values were similar in phases I and II, with absolute accuracy as follow: $A_{RMS} \pm 5.3\%$, mean bias 0.0%, precision 5.3%, and limits of agreement −10% to 10% (Table 3; Figs 1, 2). Of the sensors, 53% were adhesive (8004CB) and 47% were nonadhesive (8004CB-NA). The A_{RMS} accuracy and mean bias of the 8004CB and 8004CB-NA sensors were ±5.0 and ±0.3 and ±5.3 and ±1.5, respectively. There was no statistically significant difference in accuracy between these 2 sensors (95% confidence interval −1.6 to 5). The $SavO_2$ and $rScO_2$ varied widely among patients, ranging from 26% to 91% and from 34% to 91%, respectively. In the regression, the line of identity appears to bisect the data, revealing similar correlation between the variables over this wide range.

Bland-Altman analysis of agreement between $rScO_2$ and $SavO_2$ demonstrated random scatter around the horizontal line at a mean difference of zero, with no more than 5% of points outside the lines representing mean ± 2 standard deviations, and the slope of a linear regression through it was not detected to be different from zero (p value = 0.3692). There is also constant error variance across the range of saturations (Breusch-Pagan p value = 0.0762). Therefore, a single accuracy statistic (A_{RMS}) is constant over this wide range of oxygenation as supported by Bland-Altman analysis.

Comment

Cerebral hypoxia-ischemia accounts for many neurocognitive and behavioral disabilities in children with CHD. Neurologic examination, magnetic resonance imaging, jugular bulb oximetry, and electroencephalography have limited applicability for detection of hypoxia-ischemia. NIRS monitors cerebral oxygenation and can detect cerebral hypoxia-ischemia at the bedside noninvasively. Our study evaluated an advanced technology NIRS device using a single common sensor in a diverse population of pediatric patients with CHD. The device was accurate for absolute cerebral oxygen saturation over a wide range of oxygenation and ages, suggesting a role in the perioperative care of children with CHD.

Since the introduction of NIRS many years ago, it has evolved, been commercialized, and is being applied clinically [18]. Advances in physics, optical technologies, methods to calibrate and validate the NIRS measurement [11–13], and animal models to identify threshold $rScO_2$ for hypoxia-ischemia have contributed to its clinical application [8, 10].

The principles behind NIRS are fundamentally similar to pulse oximetry. As light passes through tissue, it is absorbed and scattered. Oxyhemoglobin and deoxyhemoglobin mainly absorb the light while other compounds (eg, water, cytochromes) absorb to a less extent. Light is scattered by tissue interfaces and cellular particulates that vary with age and brain tissue maturation [19]. To accurately measure oxyhemoglobin and deoxyhemoglobin to calculate $rScO_2$, it is necessary to account for

Table 1. Subject Demographic Characteristics

Variable	Phase I (n = 41 subjects)	Phase II (n = 45 subjects)	Both Phases (n = 86 Subjects)
Age (years)	1.0 (41) [0.0–11.0]	0.0 (45) [0.0–10.0]	0.0 (86) [0.0–11.0]
Age			
Neonate (0–30 days)	2/41 (5%)	5/45 (11%)	7/86 (8%)
Infant (31 days–2 years)	23/41 (56%)	21/45 (47%)	44/86 (51%)
Pediatric (2–12 years)	16/41 (39%)	19/45 (42%)	35/86 (41%)
Gender			
Male	16/41 (39%)	23/45 (51%)	39/86 (45%)
Female	25/41 (61%)	22/45 (49%)	47/86 (55%)
Race			
American Indian or Alaska Native	1/41 (2%)	0/45 (0%)	1/86 (1%)
Asian	2/41 (5%)	3/45 (7%)	5/86 (6%)
Black or African American	2/41 (5%)	7/45 (16%)	9/86 (11%)
White	36/41 (88%)	32/45 (71%)	68/86 (79%)
Other	0/41 (0%)	4/45 (9%)	4/86 (5%)
Weight (kg)	8.6 (41) [2.6–39.8]	8.3 (45) [2.4–30.8]	8.4 (86) [2.4–39.8]
Head circumference (inches)	44.4 (39) [31.0–54.0]	43.6 (45) [32.0–54.5]	44.0 (84) [31.0–54.5]
Gestational age (weeks)	39.5 (14) [32–41]	38.0 (16) [25–40]	38.5 (30) [25–41]
Skin tone			
Very light	6/41 (15%)	8/45 (18%)	14/86 (16%)
Light	26/41 (63%)	21/45 (47%)	47/86 (55%)
Light intermediate	5/41 (12%)	9/45 (20%)	14/86 (16%)
Dark intermediate	2/41 (5%)	3/45 (7%)	5/86 (6%)
Dark	2/41 (5%)	4/45 (9%)	6/86 (7%)
Room air SpO_2 (%)			
[70–80)	3/41 (7%)	11/44 (25%)	14/85 (17%)
[80–90)	6/41 (15%)	15/44 (34%)	21/85 (25%)
[90–100]	32/41 (78%)	18/44 (41%)	50/85 (59%)
Bilirubin (mg/mL)	2.3 (3) [0.2–6.2]	1.8 (2) [0.5–3.1]	2.1 (5) [0.2–6.2]

Data presented as number of observations/number of subjects (%) or median (number of observations) [minimum, maximum].

SpO_2 = air pulse oximetry.

absorption and light scattering by other compounds, which requires a device construct utilizing at least 3 wavelengths and 2 source-detector separations. Accuracy is improved by using more wavelengths, more source-detector separations, or both.

The Covidien and CASMED NIRS devices are FDA cleared and currently being used to measure $rScO_2$ in children with CHD. The Covidien device utilizes a single 2 wavelength emitter and 2 detectors located at 3 and 4 cm from the emitter, a construct not permitting measurement of absolute $rScO_2$ [20]. This device, evaluated in 31 patients with CHD undergoing cardiac catheterization ranging in age from 1 month to 16 years, compared $rScO_2$ against SjO_2 [19]. The device mean bias was 5.2% with limits of agreement between 8.4% and 18.8% for $rScO_2$ compared with SjO_2 [19]. As expected from the construct, large bias and wide limits of agreement, the Covidien device does not accurately measure absolute $rScO_2$. Correlation between $rScO_2$ and SjO_2 permits the device to monitor changes in cerebral oxygenation and be used in this capacity at many pediatric centers. The CASMED company introduced a neonatal sensor utilizing a single 3 wavelength emitter and 1 detector 2.5 cm apart. The device was validated in 17 neonates undergoing ECMO in which $rScO_2$ was compared against SjO_2 [11]. The device had a mean bias of 0.4%, precision of $\pm$5.1%, and limits of agreement $-$10% to 10% compared with SjO_2 [11]. Thus, the device accurately measures absolute $rScO_2$ although only validated in a narrow range of patient age and oxygenation, raising concerns about its accuracy beyond the neonatal age. Subsequently, CASMED introduced a pediatric sensor using 4 wavelengths and 2 detectors with source-detector separations of 1.5 and 4.0 cm. The performance of this device was not available in peer-reviewed literature.

The Nonin device also detects absolute cerebral oxy-

Table 2. Arterial and Venous Co-Oximeter Results

Lab Value (Units)	Arterial			Venous		
	Phase I (n = 41 Subjects)	Phase II (n = 45 Subjects)	Both Phases (n = 86 Subjects)	Phase I (n = 41 Subjects)	Phase II (n = 45 Subjects)	Both Phases (n = 86 Subjects)
pH	7.4 (40) [7.2–7.5]	7.4 (44) [7.2–7.5]	7.4 (84) [7.2–7.5]	7.3 (40) [7.2–7.4]	7.3 (43) [7.0–7.5]	7.3 (83) [7.0–7.5]
P_{CO_2} (mm Hg)	41.3 (40) [28.5–61.2]	38.5 (44) [29.2–55.9]	38.9 (84) [28.5–61.2]	49.6 (40) [36.4–69.4]	45.8 (43) [36.4–63.5]	47.3 (83) [36.4–69.4]
P_{O_2} (mm Hg)	72.7 (40) [34.9–131.4]	51.9 (41) [25.3–117.0]	62.8 (81) [25.3–131.4]	37.9 (40) [21.4–58.5]	34.6 (41) [21.1–54.6]	36.3 (81) [21.1–58.5]
Hct (%)	32.5 (40) [24.0–52.0]	37.0 (45) [24.0–69.0]	35.0 (85) [24.0–69.0]	33.0 (41) [24.0–53.0]	36.0 (45) [24.0–68.0]	34.0 (86) [24.0–68.0]
tHb (g/dL)	11.1 (40) [8.1–17.8]	12.5 (45) [8.2–23.3]	11.9 (85) [8.1–23.3]	11.2 (41) [8.1–17.9]	12.1 (45) [8.2–23.0]	11.6 (86) [8.1–23.0]
COHb (%)	0.5 (40) [0.2–0.9]	0.5 (45) [0.3–0.8]	0.5 (85) [0.2–0.9]	0.7 (41) [0.2–1.9]	0.7 (45) [0.1–1.6]	0.7 (86) [0.1–1.9]
MetHb (%)	0.8 (40) [0.0–1.5]	1.0 (45) [0.2–1.9]	0.9 (85) [0.0–1.9]	0.8 (41) [0.1–2.3]	1.0 (45) [0.2–2.8]	0.9 (86) [0.1–2.8]
S_{O_2} (%)	94.2 (41) [69.8–100]	87.9 (45) [34.4–98.6]	91.8 (86) [34.4–100]	65.3 (41) [35.4–88.0]	60.9 (45) [23.0–88.6]	63.0 (86) [23.0–88.6]

Data presented as median (number of observations) [minimum, maximum].

COHb = carboxyhemoglobin; Hct = hematocrit; MetHb = methemoglobin; P_{CO_2} = partial pressure of carbon dioxide; P_{O_2} = partial pressure of oxygen; S_{O_2} = oxygen saturation; tHb = total hemoglobin.

gen saturation and offers the advantage of having one common sensor accurate in a wide range of pediatric patients (ages 4 days to 11 years) over a wide range of cerebral oxygen saturations (26% to 91%). The construct of the Nonin device uses 4 wavelengths and emitter-detector separations. This dual-emitter/dual-detector sensor architecture, along with a dynamic compensatory algorithm, better eliminates scalp and skull tissue contamination to focus on brain tissue and accounts for variation in light scattering associated with age, brain development, and cerebral vasodilation to permit accuracy over a wide range of patient demographics and conditions.

How accurate must a NIRS device be to diagnose cerebral hypoxia-ischemia? In healthy neonates, infants, children, and adults and animals, $rScO_2$ ranges from 60% to 80%. In infant piglet models of cerebral hypoxia-ischemia, neurophysiologic function begins to

Table 3. Absolute $rScO_2$ Accuracy Information by Laterality

Variable	Phase I (n = 41 subjects)	Phase II (n = 45 subjects)	Both Phases (n = 86 Subjects)
Ipsilateral			
A_{RMS}[a]	4.6 (3.50–7.16)	5.9 (4.74–7.31)	5.3 (4.48–6.47)
Mean bias[b]	0.9 ± 4.52 (41) [−7.5–17.3]	−0.7 ± 5.84 (45) [−15.1–12.2]	0.0 ± 5.31 (86) [−15.1–17.3]
Precision[a]	4.58 (3.73–5.81)	5.90 (4.85–7.39)	5.34 (4.63–6.26)
Intercept[a]	11.87 (1.52–22.22)	12.91 (3.32–22.50)	11.00 (4.08–17.92)
Slope[a]	0.85 (0.71–0.99)	0.80 (0.66–0.94)	0.85 (0.75–0.94)
R[a]	0.89 (0.805–0.941)	0.87 (0.777–0.928)	0.88 (0.828–0.924)
Contralateral			
A_{RMS}[a]	4.2 (3.42–5.22)	6.5 (5.18–8.30)	5.5 (4.63–6.69)
Mean bias[b]	1.6 ± 3.91 (41) [−7.1–9.8]	0.6 ± 6.48 (42) [−16.1–15.4]	1.1 ± 5.39 (83) [−16.1–15.4]
Precision[a]	3.96 (3.23–5.03)	6.56 (5.36–8.29)	5.42 (4.69–6.37)
Intercept[a]	12.71 (3.95–21.46)	18.33 (8.03–28.63)	15.11 (8.29–21.93)
Slope[a]	0.85 (0.73–0.97)	0.74 (0.59–0.89)	0.80 (0.71–0.90)
R[a]	0.92 (0.852–0.956)	0.85 (0.733–0.916)	0.88 (0.823–0.922)

[a] Data presented as estimate (lower 95% confidence limit; upper 95% confidence limit). [b] Data presented as mean ± standard deviation (number of observations) [minimum, maximum]. Standard deviation is presented with a denominator of N to allow calculation of A_{RMS} from Mean bias and standard deviation.

A_{RMS} = accuracy root mean square; R = Pearson correlation coefficient; $rScO_2$ = regional cerebral oxygen saturation.

deteriorate at $rScO_2$ of 45% and brain injury increases hourly at $rScO_2$ less than 40% [8, 10]. Thus, there is a 15% to 20% $rScO_2$ buffer between normal and cerebral hypoxia-ischemia. In infants with CHD, the threshold is uncertain and is likely to vary with the type of CHD and level of adaptation to hypoxia. For example, an infant with a normal $rScO_2$ and noncyanotic heart disease may have a threshold of 45%, whereas a child with cyanotic heart disease may have a lower threshold because of adaptive mechanisms to hypoxia. Given this possible scenario, it is not surprising that one study found evidence for a threshold $rScO_2$ of 45% [21], whereas another study did not [22]. Nevertheless, if the concept of a buffer and a threshold exists and is similar to animal studies, then the NIRS device would need a precision of 5% to yield confidence intervals of 15% irrespective of the exact threshold. The Nonin NIRS device was developed and validated for this level of accuracy.

Limitations of this study include the uncertainties and variability in the use of $SavO_2$ to compare $rScO_2$ against, and the range of oxygenation and conditions of the patients. The arterial to venous ratio in the cerebral circulation may not be exactly 30:70 in all patients. Using a value other than 0.70 would shift $rScO_2$ versus $SavO_2$ calibration slightly (<5%), but would not significantly change the accuracy or A_{RMS}. Thus, a component of the imprecision of the NIRS measurement rests in $SavO_2$. There were only 2 patients with very low cerebral saturation (ie, $rScO_2 < 45\%$) so the device performance under extreme conditions was not thoroughly evaluated. Although the accuracy of the values at low cerebral saturation (<45%) is less certain, any low value is concerning as cerebral function is disturbed and at risk for cerebral hypoxia-ischemia. Therapies to increase $rScO_2$ include adjustments to inspired oxygen, minute ventilation, arterial pressure, and hemoglobin concentration [23].

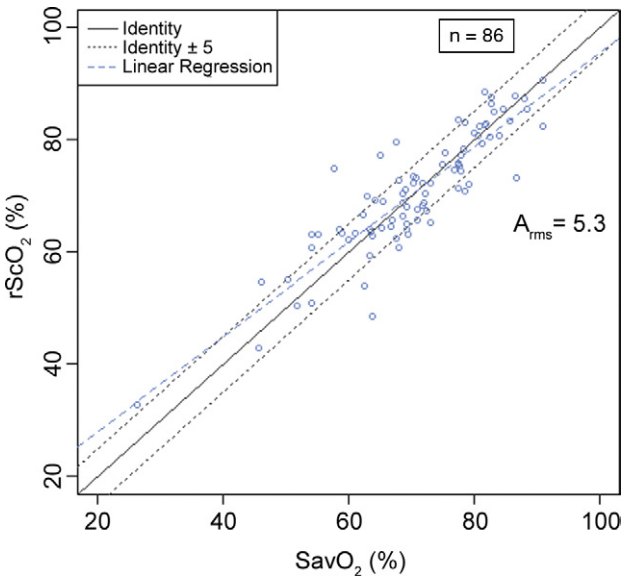

Fig 1. Ipsilateral $rScO_2$ versus SavO2 in both phases (n = 86). Equanox 8004CB cerebral $rScO_2$ and $SavO_2$ calculated from jugular venous and arterial blood samples with the line of identity provided for reference with dashed lines representing 5% above and below. Data are centered around the line of identity indicating agreement between measures. (A_{RMS} = accuracy root mean square; $rScO_2$ = regional cerebral oxygen saturation; $SavO_2$ = arteriovenous oxygen saturation.)

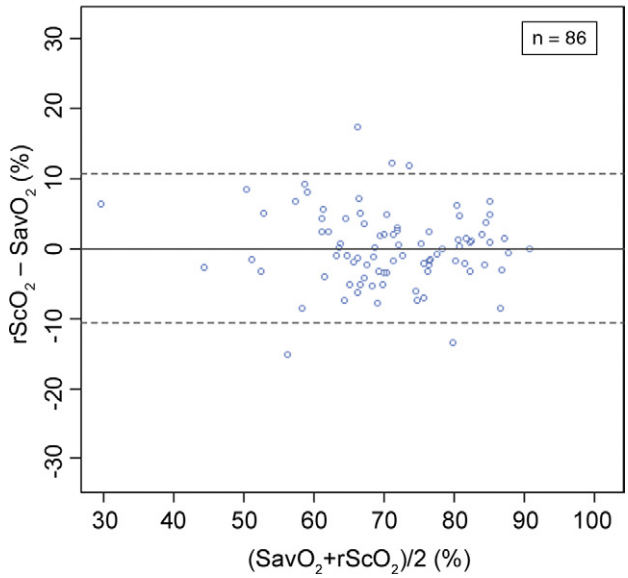

Fig 2. Bland-Altman plot of ipsilateral rScO2 in both phases (n = 86). Bland-Altman plot for absolute accuracy of the 8004CB sensor, where the difference between each $rScO_2$ and the corresponding $SavO_2$ was determined and plotted against the average of the 2 values. Dashed lines represent the lines of agreement. Lack of pattern indicates consistent accuracy across the range of $SavO_2$ saturations. ($rScO_2$ = regional cerebral oxygen saturation; $SavO_2$ = arteriovenous oxygen saturation.)

Mortality and complication rates after congenital cardiac surgery have decreased over the years [1–3]. However, subsets of children continue to experience neurocognitive and behavioral disabilities. Prevention or minimization of these disabilities demands increased attention as more children with CHD live longer. The NIRS technology may provide a window into the status of cerebral oxygenation and provide the clinician with the opportunity to intervene before permanent injury occurs.

We would like to thank Aaron Lobbestael, Shelia Salisbury, Lindsay Schultz, Kristin Miller, Eileen Beckman, Archana Verma, Lisa Jones, Erlinda Yeh, and Mary Heitschmidt for their assistance.

Financial support for the study was provided in part by Nonin Medical, Inc. Trial registration #: NCT00939224. All participating centers borrowed all study materials from Nonin Medical, Inc. Authors were given full control of study design, methods, outcome parameters and results, data analysis, and production of the written report.

References

1. Domi T, Edgell DS, McCrindle BW, et al. Frequency, predictors and neurologic outcomes of vaso-occlusive strokes as-

sociated with cardiac surgery in children. J Pediatr 2008;122:1292–8.
2. Menache C, duPlessis AJ, Wessel DL, Jonas RA, Newburger JW. Current incidence of acute neurologic complications after open-heart operations in children. Ann Thorac Surg 2002;73:1752–8.
3. Ferry P. Neurologic sequelae of open-heart surgery in children. An 'irritating question.' Am J Dis Child 1990;44:369–73.
4. Ballweg JA, Wernovsky G, Gaynor JW. Neurodevelopmental outcomes following congenital heart surgery. Pediatr Cardiol 2007;28:126–33.
5. Nioka S, Chance B, Smith DS, et al. Cerebral energy metabolism and oxygen state during hypoxia in neonate and adult dogs. Pediatr Res 1990;28:54–62.
6. Brun NC, Moen A, Borch K, Suagstad OD, Greisen G. Near-infrared monitoring of cerebral tissue oxygen saturation and blood volume in newborn piglets. Am J Physiol 1997;273(2 Pt 2):H682–6.
7. Tsuji M, duPlessis A, Taylor G, Crocker R, Volpe JJ. Near infrared spectroscopy detects cerebral ischemia during hypotension in piglets. Pediatr Res 1998;44:591–5.
8. Kurth CD, Levy WJ, McCann JC. Near-infrared spectroscopy cerebral oxygen saturation thresholds for hypoxia-ischemia in piglets. J Cereb Blood Flow Metab 2002;22:335–41.
9. Ferrari M, Mottola L, Quaresima V. Principles, techniques, and limitations of near infrared spectroscopy. Can J Appl Physiol 2004;29:463–87.
10. Kurth CD, McCann JC, Wu J, Miles L, Loepke AW. Cerebral oxygen saturation time thresholds for cerebral hypoxia-ischemia injury in piglets. Anesth Analg 2009;108:1268–77.
11. Rais-Bahrami K, Rivera O, Short BL. Validation of a noninvasive neonatal optical cerebral oximeter in veno-venous ECMO patients with a cephalad catheter. J Perinatol 2006;26:628–35.
12. Watzman HM, Kurth CD, Montenegro LM, Rome J, Steven JM, Nicolson SC. Arterial and venous contributions to near-infrared cerebral oximetry. Anesthesiology 2000;93:947–53.
13. Nelson LA, McCann JC, Loepke AW, Wu J, Kurth CD. Development and validation of a multiwavelength spatial domain near-infrared oximeter to detect cerebral hypoxia-ischemia. J Biomed Opt 2006;11:064022.
14. Efron B, Tibshirani R. An introduction to the bootstrap. Boca Raton, FL: CRC Press LLC; 2000.
15. Lehmann EL. Testing statistical hypotheses. 1986: New York: John Wiley & Sons.
16. Bland JM, Altman DG. Agreement between methods of measurement with multiple observations per individual. J Biopharm Stat 2007;17:571–82.
17. Bland JM, Altman DG. Statistical methods for assessing agreement between two methods of clinical measurement. Lancet 1986;1:307–10.
18. Jöbsis FF. Noninvasive, infrared monitoring of cerebral and myocardial oxygen sufficiency and circulatory parameters. Science 1977;198:1264–7.
19. van der Zee P, Essenpreis ME, Delpy DT. Optical properties of brain tissue. Proc. SPIE 1888:454–65.
20. Nagdyman N, Ewert P, Peters B, Miera O, Fleck T, Berger F. Comparison of different near-infrared spectroscopic cerebral oxygenation indices with central venous and jugular venous oxygenation saturation in children. Paediatr Anaesth 2008;18:160–6.
21. Dent CL, Spaeth JP, Jones BV, et al. Brain magnetic resonance imaging abnormalities after the Norwood procedure using regional cerebral perfusion. J Thorac Cardiovasc Surg 2006;131:190–7.
22. Kussman BD, Wypij D, DiNardo JA, et al. Cerebral oximetry during infant cardiac surgery: evaluation of and relationship to early postoperative outcome. Anesth Analg 2009:108:1122–31.
23. Andropoulos DB, Stayer SA, Diaz LK, Ramamoorthy C. Neurological monitoring for congenital heart surgery. Anesth Analg 2004;99:1365–75.